

Supplemental Information

Understanding the CH₄ Conversion over Metal Dimers from First Principles

Haihong Meng ¹, Bing Han ¹, Fengyu Li ^{1,*}, Jingxiang Zhao ^{2,*} and Zhongfang Chen ^{3,*}

¹ School of Physical Science and Technology, Inner Mongolia University, Hohhot 010021, China; dundun_0521@163.com (H.M.); binghan1214@163.com (B.H.)

² College of Chemistry and Chemical Engineering, Key Laboratory of Photonic and Electronic Bandgap Materials, Ministry of Education, Harbin Normal University, Harbin 150025, China

³ Department of Chemistry, The Institute for Functional Nanomaterials, University of Puerto Rico, Rio Piedras Campus, San Juan, PR 00931, USA

* Correspondence: fengyuli@imu.edu.cn (F.L.); xjz_hmily@163.com (J.Z.); zhongfangchen@gmail.com (Z.C.)

Table S1. The lattice parameters (a/b , in Å) of M₂-Pc catalysts, their corresponding bond lengths (the bond lengths of metal to metal, metal to nitrogen, d_{M-M} , d_{M-N} , d_{M-Nc} , where Nc represents the N atom adjacent to the C atom, in Å), and the binding energy (E_b , in eV) of metal dimer anchoring at Pc monolayer, as well as the cohesive energy (E_{bulk} , in eV) of metal in bulk.

M	$a/\text{\AA}$	$b/\text{\AA}$	$d_{M-M}/\text{\AA}$	$d_{M-N}/\text{\AA}$	$d_{M-Nc}/\text{\AA}$	E_b/eV	E_{bulk}/eV
Sc	14.19	14.26	2.95	2.08	2.05	-11.50	-6.20
Ti	14.16	14.22	2.66	2.02	1.94	-12.15	-7.76
V	14.13	14.18	2.56	2.00	1.90	-11.29	-9.76
Cr	14.23	14.25	2.52	1.94	1.86	-9.66	-9.49
Mn	14.18	14.19	2.38	1.95	1.82	-9.66	-8.94
Fe	14.13	14.14	2.33	1.93	1.78	-10.06	-8.30
Co	14.10	14.12	2.37	1.91	1.77	-10.52	-7.11
Ni	14.17	14.18	2.73	1.83	1.83	-9.92	-5.57
Cu	14.23	14.25	2.82	1.86	1.89	-7.26	-4.39
Zn	14.21	14.27	2.84	1.93	1.98	-5.04	-1.26
Y	14.18	14.25	3.25	2.22	2.22	-11.05	-6.32
Zr	14.22	14.27	2.95	2.12	2.08	-12.49	-8.48
Nb	14.17	14.23	2.57	2.11	2.00	-12.11	-10.22
Mo	14.16	14.22	2.50	2.06	1.96	-10.21	-10.95
Ru	14.26	14.28	2.43	2.00	1.91	-11.42	-9.20
Rh	14.27	14.28	2.49	1.98	1.90	-10.52	-7.26
Pd	14.23	14.30	2.84	1.94	1.98	-7.60	-5.16
Ag	14.25	14.31	2.79	1.99	2.06	-4.13	-3.37
Hf	14.21	14.27	2.94	2.08	2.05	-13.17	-9.96
Ta	14.19	14.25	2.72	2.07	2.01	-13.47	-11.86
W	14.18	14.22	2.52	2.05	1.97	-12.63	-13.01
Re	14.26	14.28	2.40	2.01	1.94	-12.06	-12.00
Os	14.24	14.25	2.42	1.98	1.92	-12.68	-11.24
Ir	14.27	14.28	2.51	1.98	1.92	-12.06	-8.85
Pt	14.25	14.32	2.89	1.93	1.97	-9.95	-6.04
Au	14.26	14.32	2.86	1.97	2.2	-5.84	-4.46
Al	14.21	14.23	2.71	1.86	1.85	-10.58	-5.52
Ga	14.29	14.31	2.78	1.90	1.90	-7.54	-3.45
Sn	14.18	14.25	3.27	2.29	2.23	-6.71	-4.38
Bi	14.18	14.26	3.33	2.25	2.24	-5.95	-4.68

Table S2a. The reaction energy for H₂O₂ dissociation into *O + H₂O on the M₂-Pc (M = Sc, Zr, Nb, W), bond lengths of two metal atoms with oxygen (d_{M1-O}/d_{M2-O} , in Å) (M1 = M2 = M), as well as the H₂O binding energies ($E_{ads(H2O)}$, in eV).

	$\Delta E/\text{eV}$	$d_{M1-O}/\text{\AA}$	$d_{M2-O}/\text{\AA}$	$E_{ads(H2O)}/\text{eV}$
Sc	-27.12	1.98	1.97	-0.31
Zr	-26.83	2.05	2.05	-0.21
Nb	-25.91	2.00	2.00	-0.27

W	-23.52	2.06	1.96	-0.13
---	--------	------	------	-------

Table S2b. The reaction energy for H_2O_2 dissociation into $*\text{OH} + *\text{OH}$ on the $\text{M}_2\text{-Pc}$ ($\text{M} = \text{Sc}, \text{Ti}, \text{V}, \text{Y}, \text{Zr}, \text{Hf}, \text{Ta}, \text{W}$), as well as the bond lengths ($d_{\text{M1}-\text{O}}/d_{\text{M2}-\text{O}}, d_{\text{O1}-\text{O2}}, d_{\text{O1}-\text{H}}/d_{\text{O2}-\text{H}}, \text{\AA}$) ($\text{M1} = \text{M2} = \text{M}$), O1 and O2 represent the two O atoms bonded to M1 and M2, respectively.

	$\Delta E/\text{eV}$	$d_{\text{M1}-\text{O}}/\text{\AA}$	$d_{\text{M2}-\text{O}}/\text{\AA}$	$d_{\text{O1}-\text{O2}}/\text{\AA}$	$d_{\text{O1}-\text{H}}/\text{\AA}$	$d_{\text{O2}-\text{H}}/\text{\AA}$
Sc	-5.19	1.93	1.92	2.99	0.97	0.97
Ti	-7.51	1.83	1.83	2.93	0.97	0.97
V	-6.70	1.79	1.79	2.98	1.03	0.98
Y	-5.03	2.08	2.07	3.10	0.97	0.97
Zr	-8.16	2.00	1.99	3.18	0.97	0.97
Hf	-8.71	1.95	1.96	2.97	0.97	0.97
Ta	-9.04	1.91	1.91	3.02	0.97	0.97
W	-7.41	1.95	1.88	2.76	1.00	0.98

Table S3. The total magnetic moments and magnetic moment (in μ_B) on the two metal atoms of the $\text{M}_2\text{-Pc}$ ($\text{M} = \text{Sc}, \text{Ti}, \text{V}, \text{Y}, \text{Zr}, \text{Nb}, \text{Hf}, \text{Ta}, \text{W}$) (structures were shown in Figure S2), and the Bader charge (q , in $|e|$) of the two atoms.

	total	M1	M2	q_{M1}	q_{M2}
Nb	0.93	0.37	0.37	1.72	1.71
Sc	0.00	0.00	0.00	+1.86	+1.86
Ta	-0.02	0.45	-0.50	+1.79	+1.79
Ti	0.77	0.44	0.44	+1.78	+1.78
V	3.16	1.60	1.60	+1.57	+1.57
Y	0.00	0.00	0.00	+1.98	+1.98
Zr	0.39	0.22	0.22	+1.98	+1.98
Hf	0.39	0.20	0.20	+1.98	+1.98
W	0.00	0.69	-0.69	+1.60	+1.60

Table S4. The calculated zero-point energy, entropy, and free energy change of the reaction of the abstraction of a hydrogen from one of the $^*\text{OH}$ groups to the formation of water and oxo species ($^*\text{OH} + ^*\text{OH} \rightarrow * \text{O} + \text{H}_2\text{O}$) on $\text{M}_2\text{-Pc}$ ($\text{M} = \text{Ti}, \text{V}, \text{Y}, \text{Hf}, \text{Ta}$).

	2^*OH		$^*\text{O} + \text{H}_2\text{O}$		$\Delta G/\text{eV}$
	ZPE	$T^*\Delta S$	ZPE	$T^*\Delta S$	
Ti	0.65	0.21	0.67	0.25	0.91
V	0.69	0.21	0.74	0.16	0.74
Y	0.68	0.23	0.74	0.17	1.83
Hf	0.72	0.12	0.76	0.14	1.72
Ta	0.63	0.20	0.69	0.11	1.63

Table S5. The calculated zero-point energy, entropy, and free energy change of the self-reaction of H_2O_2 ($2^*\text{OH} + \text{H}_2\text{O}_2 \rightarrow \text{O}_2 + 2\text{H}_2\text{O}$) on $\text{M}_2\text{-Pc}$ ($\text{M} = \text{Sc}, \text{Ti}, \text{V}, \text{Y}, \text{Zr}, \text{Hf}$).

	$2^*\text{OH} + \text{H}_2\text{O}_2$		$\text{O}_2 + 2\text{H}_2\text{O}$		$\Delta G/\text{eV}$
	ZPE	$T^*\Delta S$	ZPE	$T^*\Delta S$	
Sc	1.43	0.40	1.39	0.45	0.54
Ti	1.45	0.42	1.41	0.45	2.61
V	1.46	0.39	1.40	0.33	2.69
Y	1.40	0.40	1.37	0.40	0.65
Zr	1.42	0.35	1.35	0.44	3.08
Hf	1.44	0.45	1.44	0.38	-0.18

Table S6. The partial charges of O (q_{O}) and M (q_{M1} and q_{M2}) for M1-O-M2 (in $|e|$) ($\text{M1} = \text{M2} = \text{Sc}, \text{Zr}, \text{Nb}, \text{W}$). Values were obtained from Bader charge analysis.

	q_{M1}	q_{M2}	q_{O}
--	-----------------	-----------------	----------------

Sc1-O-Sc2	+1.89	+1.89	-1.14
Zr1-O-Zr2	+2.30	+2.30	-1.17
Nb1-O-Nb2	+2.10	+2.08	-1.07
W1-O-W2	+1.99	+2.03	-0.94

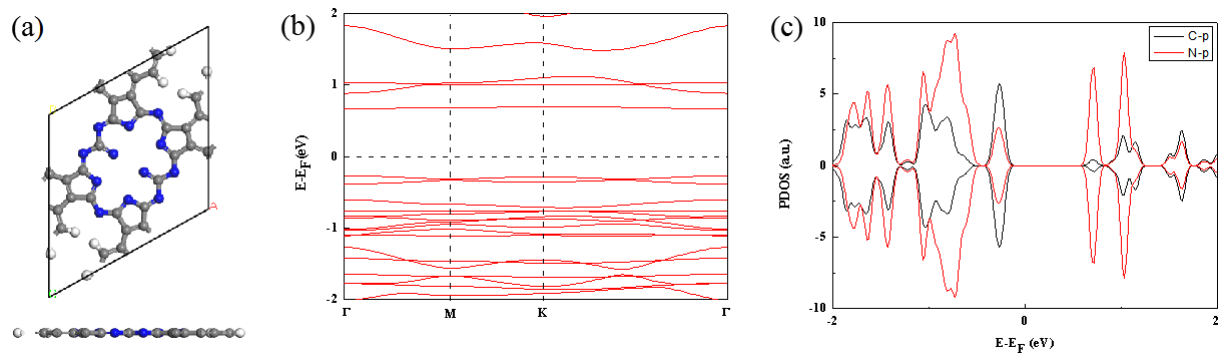


Figure S1. Top and side view of the structure of P_c in a $2 \times 2 \times 1$ supercell (a), the band structure (b) and projected density of state (PDOS) (c). The Fermi lever is set to zero.

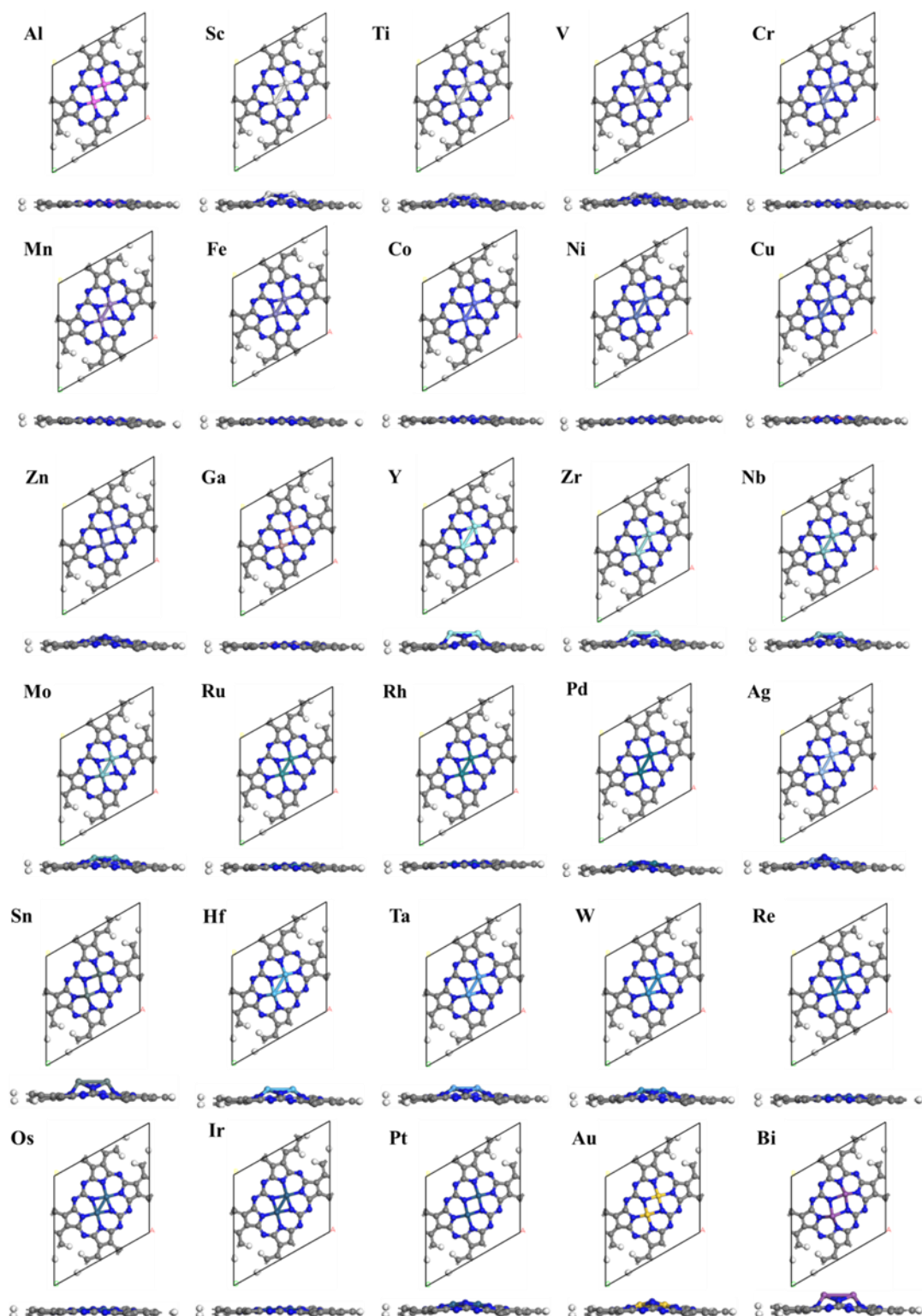


Figure S2. Top and side views of the optimized $M_2\text{-Pc}$ monolayers.

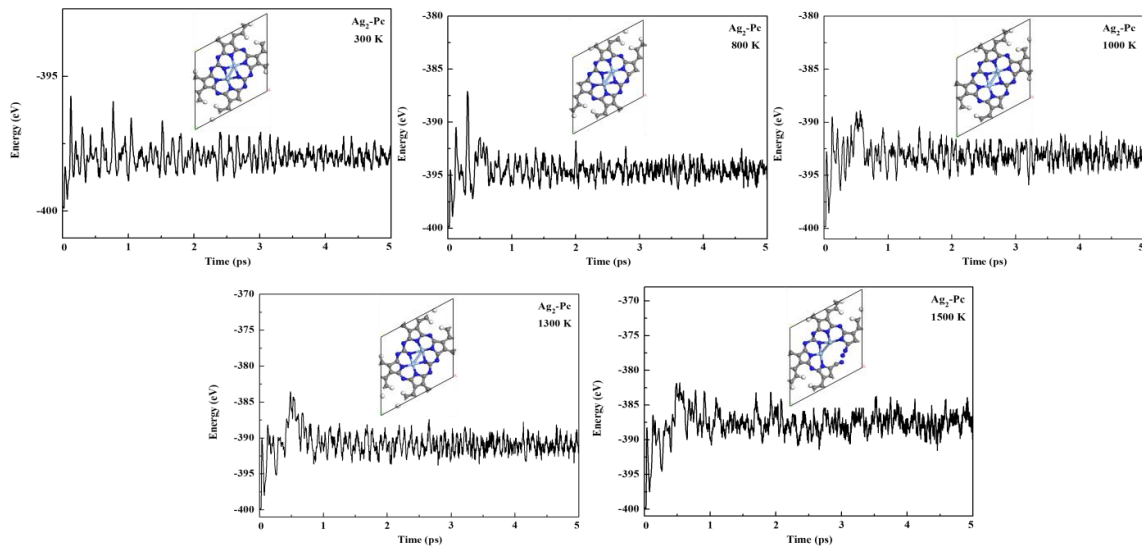


Figure S3. The energy evolution with time progress of the 5 ps FPMD simulation of the Ag₂-Pc at 300 K, 800, 1000, 1300, and 1500 K, as well as the snapshot of structure at the end of 5 ps.

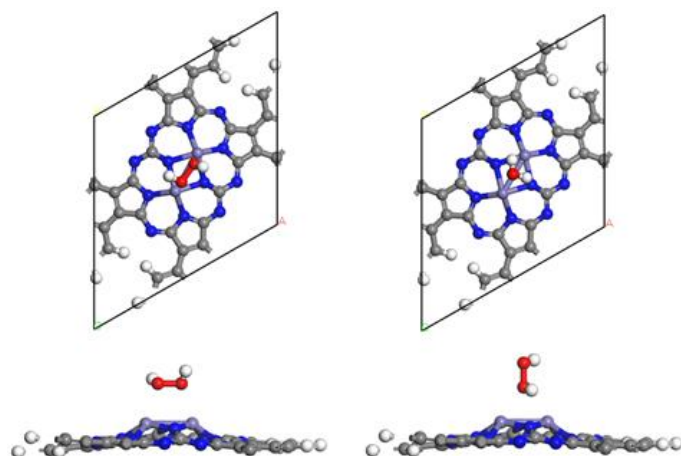


Figure S4. Two adsorption configurations of H₂O₂ on the M₂-Pc.

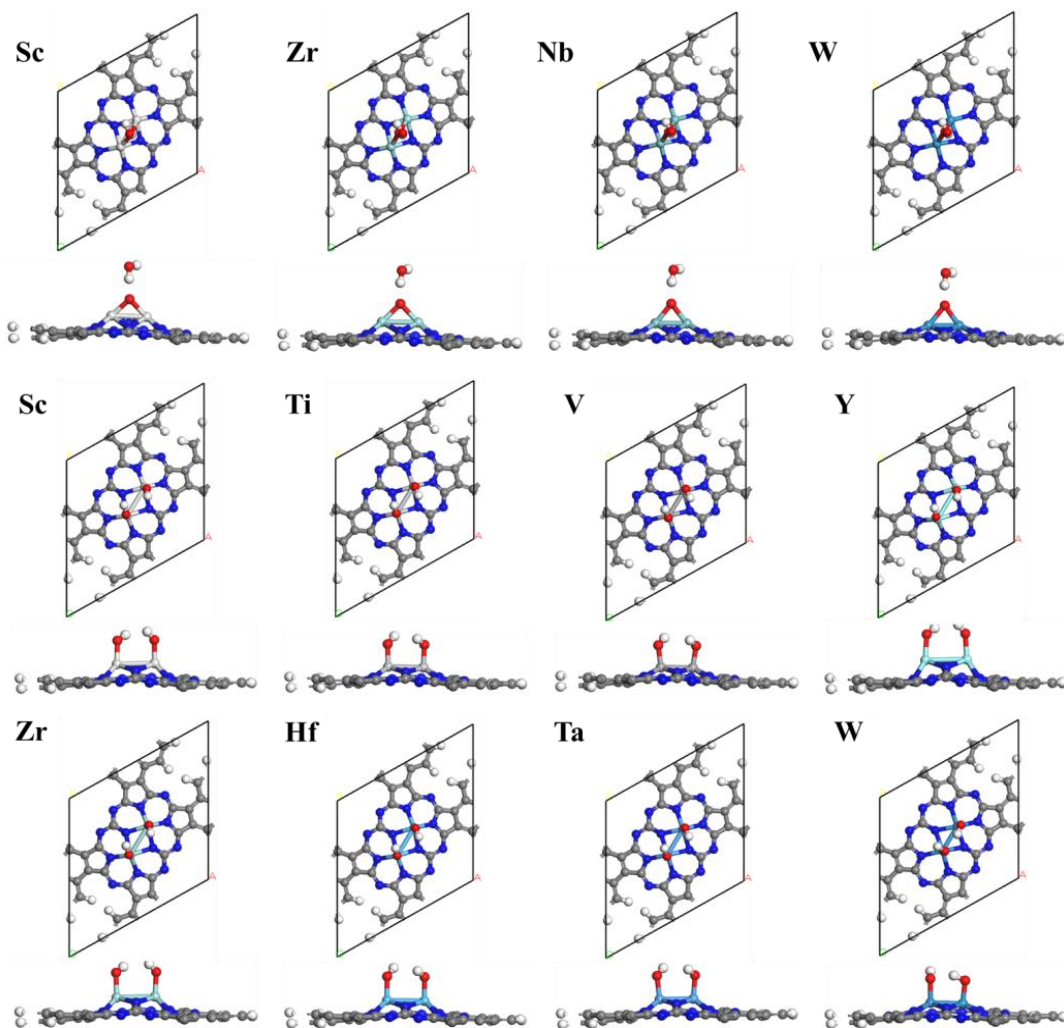


Figure S5. The structures of spontaneously dissociated H_2O_2 on the $\text{M}_2\text{-Pc}$ monolayers.

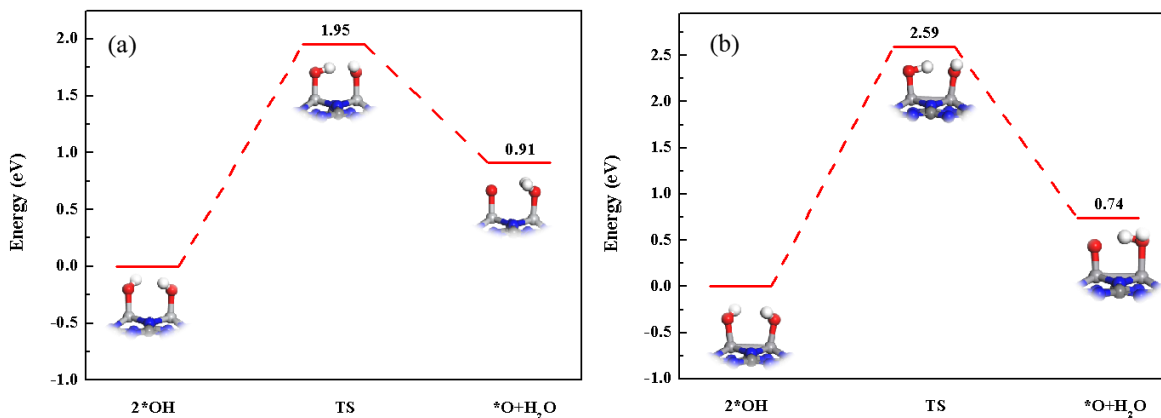


Figure S6. Transformation process of $*\text{OH} + *\text{OH} \rightarrow *\text{O} + \text{H}_2\text{O}$ on the $\text{Ti}_2\text{-Pc}$ (a) and $\text{V}_2\text{-Pc}$ (b) surfaces. The inset was the atomic structure model of each step.

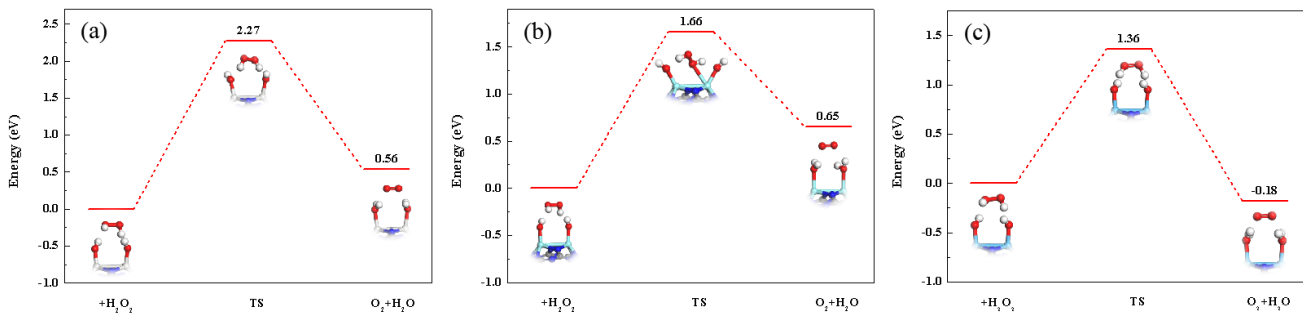


Figure S7. Transformation process of $H_2O_2 + 2(*OH) \rightarrow O_2 + 2H_2O$ on the Sc₂-Pc (a), Y₂-Pc (b), and Hf₂-Pc surface (c). The inset was the atomic structure model of each step.

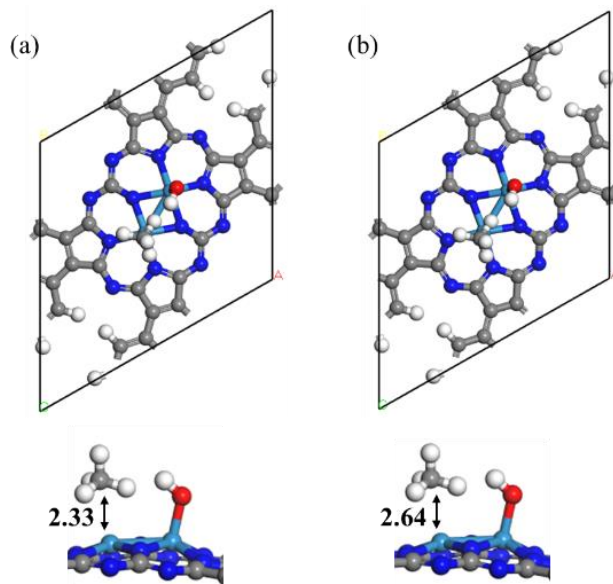


Figure S8. The initial state structure (a) and the final state structure (b) of methane adsorption on W₂-Pc surface.

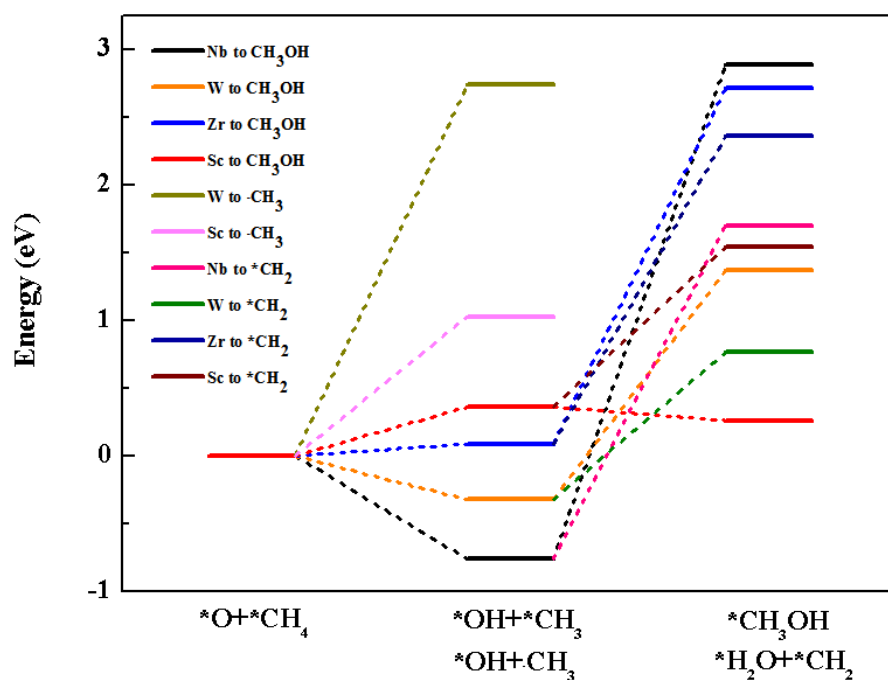


Figure S9. The corresponding energy profile of methane conversion *via* *O-assisted mechanism.

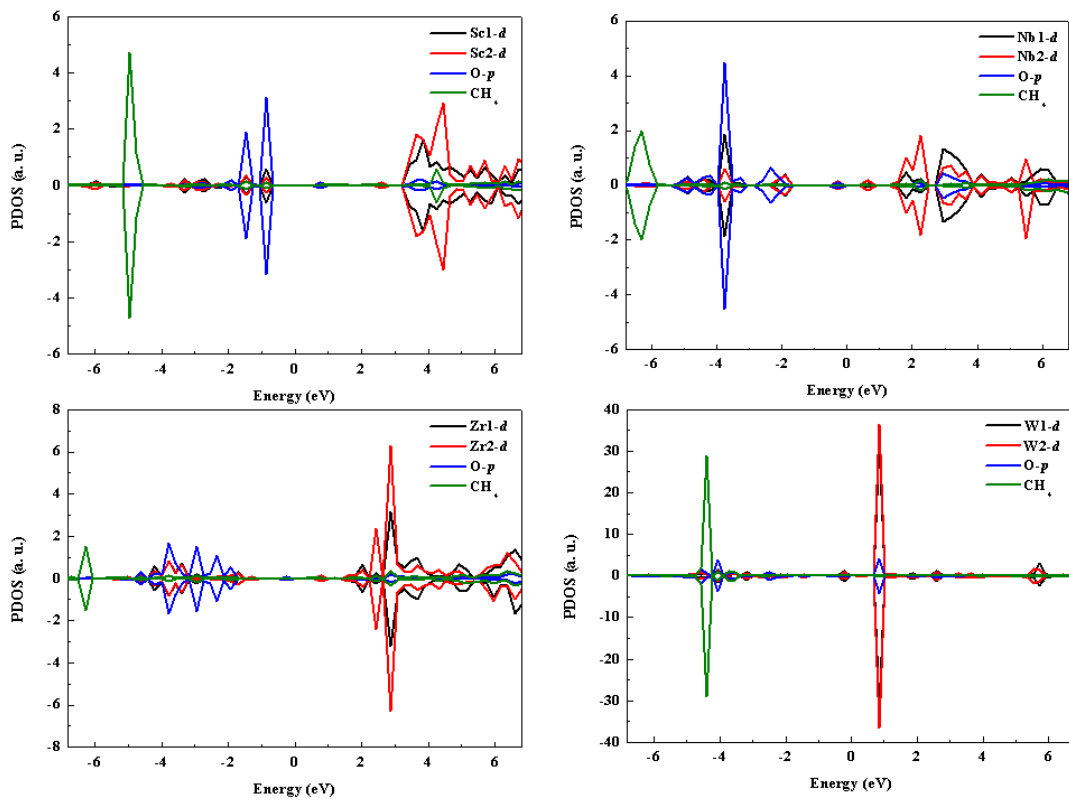


Figure S10. Partial density of states (PDOS) of CH_4 adsorption on M-O-M moiety. The Fermi level was set to zero.

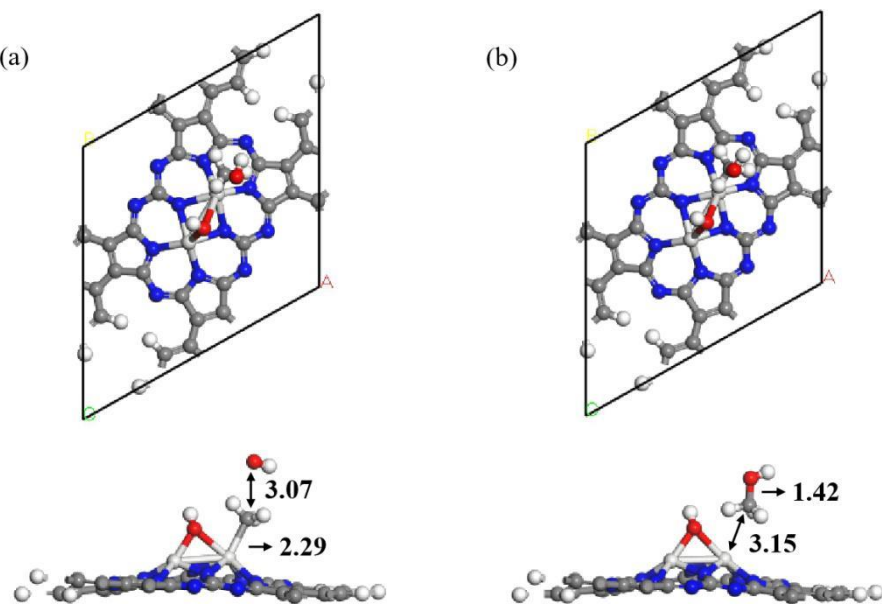


Figure S11. The initial state structure (a) and the final state structure (b) of the reaction between $^*\text{CH}_3$ and OH in solution on $\text{Sc}_2\text{-Pc}$.

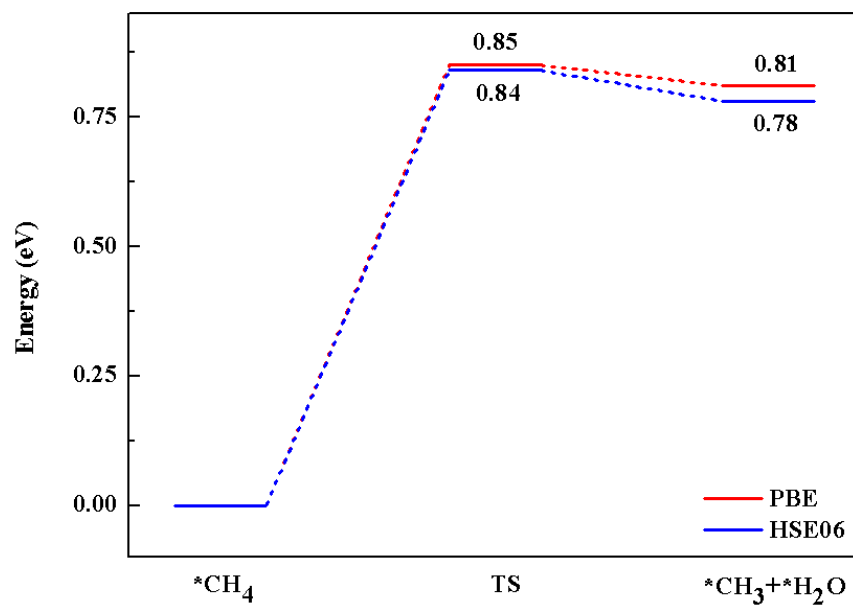


Figure S12. Energy diagram of the C–H bond cleavage on the $\text{Ti}_2\text{-Pc}$ surface calculated by PBE (red lines) and HSE06 functional (blue lines).